Volume 8, Issue 5, 2018, 3552 - 3559 ISSN 2069-5837

Biointerface Research in Applied Chemistry

www.BiointerfaceResearch.com

Original Research Article Open Access Journal

Received: 10.09.2018 / Revised: 30.09.2018 / Accepted: 04.10.2018 / Published on-line: 15.10.2018

Effects of bare and chitosan-coated Fe_3O_4 magnetic nanoparticles on seed germination and seedling growth of *Capsicum annuum* L.

Mohammad Kazem Bahrami [1], Ali Movafeghi [1, *], Gholam Reza Mahdavinia [2], Mohammad Bagher Hassanpouraghdam [3], Gholamreza Gohari [3]

[1]Department of Plant Biology, Faculty of Natural Sciences, University of Tabriz, Tabriz, Iran
[2]Department of Chemistry, Faculty of Science, University of Maragheh, Maragheh, Iran
[3]Department of Horticulture, Faculty of Agriculture, University of Maragheh, Maragheh, Iran

*corresponding author e-mail address: ***movafeghi@tabrizu.ac.ir***

ABSTRACT

In this study, the effects of different concentrations (0, 200, 400, 800, and 1600 mg/kg) of bare and chitosan(CS)-coated Fe_3O_4 magnetic nanoparticles (Fe_3O_4 MNPs) on seed germination and seedling growth of sweet pepper (*Capsicum annuum* L.) were evaluated. Bare and CS-Fe_3O_4MNPs in the size range of 3-22 nm were synthesized by co-precipitation and polyelectrolyte complex (PEC) procedures, respectively. Consequently, they were characterized using FT-IR, XRD, VSM, SEM, TEM and DLS techniques. Then, the effects of the prepared nanomaterials were evaluated on physiological parameters such as germination rate and speed, rootlet and shootlet length, fresh and dried weights as well as total iron content. It was found that bare and CS-Fe_3O_4 MNPs with concentrations of 200 and 400 mg/kg had significant impacts on seed germination and seedling growth. In addition, the higher concentrations of MNPs showed toxic effects. Taken all together, CS-Fe_3O_4 MNPs had better efficiency on the evaluated parameters in comparison to bare Fe_3O_4 MNPs.

Keywords: *Germination, Fluorescence, Seedling growth, Nanoparticle uptake.*

1. INTRODUCTION

Seed germination, creating the first vegetative structures of the plant, plays a significant role in viability, growth, development, adaptation and yield of crops [1]. During this process, seedlings gradually change their nutritional nature to photo-autotrophy. In the first stage of seed germination, the seeds absorb high amounts of water containing minerals [2]. The minerals have different influences on seed germination and seedling growth.

The traditional fertilizing methods in seedling production were reported to cause physiological stress in different plant species [1, 3]. In recent years, nanomaterials have gained growing attention in modern agriculture due to their preferential advantages such as high efficiency, reduced application frequency of fertilizer, effective bioavailability and notable biocompatibility [4-6]. Accordingly, various nanomaterials such as SiO_2, TiO_2, CuO, ZnO, and iron oxides have been utilized during seed germinations and seedling growth [7-12]. Among different nanomaterials, Fe_3O_4 magnetic nanoparticles (Fe_3O_4 MNPs) showed outstanding properties including chemical stability, electromagnetic behaviors, anti-contaminant features and low toxicity [13-16]. It is well-known that the interaction between the magnetic compounds, Fe_3O_4 MNPs, and enzymes in cells stimulates seed germination and seedling growth [4, 17-19]. Iron oxide MNPs cause the opening of root cell aquaporins resulting in more absorption of water and minerals [13]. Moreover, the concentration of magnetic nano-materials could affect the seed germination and seedling growth [20-23]. On the other hand, the concentrations of these materials have positive and negative effects depending on the plant species. For example, low concentrations of iron oxide MNPs inhibited the seed germination of Chinese bean, although they stimulated the germination in higher concentrations [13]. Seed germination of cucumber, lettuce, and oak was increased after treatment with various concentrations of Fe_3O_4 MNPs [16, 21]. In another work, different Fe_3O_4 NPs concentrations have enhanced the growth of tomato seedlings [24]. In contrary, the utilization of high concentrations of Fe_3O_4 NPs inhibited the seed germination of some plant species [25, 26].

Generally, aggregation, low stability, and toxicity of metal-based nanomaterials could be considered as the main disadvantages, upon which their applications were limited [7, 27-30]. Regarding these problems, bio-polymeric materials as coating and encapsulation agents have received recently high attention due to their biocompatibility [31, 32]. Chitosan (CS) as one of the most abundant biopolymers in nature could be prepared by N-deacetylation of chitin. It was frequently employed for the designing and encapsulation of metal nanoparticles for agricultural applications [33]. The effects of CS on the seedling growth, drought and salinity tolerance as well as resistance to infections were reported [34]. Intriguingly, the encapsulation of metal nanoparticles in biocompatible compounds such as CS biopolymer regulates the proper release of nutrients [35, 36]. For instance, chitosan coated copper nanoparticles remarkably improved maize seedling growth by up-regulating the enzymes responsible for the mobilization of stored food [37, 38]. Further, chitosan coated silver and copper nanoparticles were synthesized and their toxic effects on soil microbial status and microbial population have been studied [39]. However, the application of CS coated magnetic iron oxide nanoparticles for agricultural proposes is a new field of study.

Capsicum annuum L., a member of Solanaceae family, has high contents of antioxidant compounds and is broadly used as a valuable vegetable due to its unique properties such as anticancer and anti-inflammatory activities [40]. In the current study, bare and CS coated Fe_3O_4 MNPs were synthesized by co-precipitation and polyelectrolyte complex (PEC) methods, respectively. Synthesized materials were characterized using FT-IR, XRD, VSM, SEM, TEM and DLS techniques. The uptake of MNPs by root cells of *C. annuum* was confirmed by fluorescence microscopic images. Subsequently, the effects of prepared nanomaterials were evaluated on the seed germination, seedling growth as well as iron contents in *C. annuum*.

2. EXPERIMENTAL SECTION

2.1. Synthesis of bare and CS coated Fe_3O_4 magnetic nanoparticles.

2.1.1. Chemicals. Low molecular weight chitosan (Mw=20 kD; the degree of deacetylation= 92%) was provided from Amicogen Inc. (Jinju, South Korea). Iron salts, $FeCl_2{\cdot}4H_2O$ and $FeCl_3{\cdot}6H_2O$ were purchased from Merck Co. (Germany). Ammonia solution (25%, Merck, Germany) was used for preparing the desired dilution.

2.1.2. Synthesis of bare and CS-Fe_3O_4 MNPs. Bare Fe_3O_4 MNPs were synthesized according to the previously reported protocol [41]. In order to the synthesis of CS-Fe_3O_4 MNPs, co-precipitation of Fe^{2+}/Fe^{3+} ions through *in situ* method in presence of chitosan was accomplished. In overall, chitosan solutions were prepared by pouring 1 g of chitosan in 100 mL acetic acid solution (1% wt) at 70°C for 1 h. Then, 2 g of $FeCl_2{\cdot}4H_2O$ and 5.4 g of $FeCl_3{\cdot}6H_2O$ iron salts (nFe^{3+}/nFe^{2+} = 2) were dissolved in 20 mL of distilled water and added into the chitosan solution. The solution purged with N_2 inert gas for 30 min. Ammonia solution (3 M) was slowly dropped into (Fe^{3+}/Fe^{2+})-loaded chitosan solution until the pH of the solution reached to 11. Afterward, the formation of black Fe_3O_4 nanoparticles was observed. The magnetic solution was stirred at 70°C for 1 h. The obtained magnetic chitosan solution was thoroughly washed with excess distilled water to remove unreacted reagents. The purification was continued until the pH of the solution reached 7. To obtain a homogeneous solution, the purified magnetic chitosan sample was dispersed in 100 mL distilled water and sonicated at the frequency of 50 kHz for 30 min (Bandelin SONOPULS HD 2200). A part of purified magnetic CS-Fe_3O_4 MNPs was separated by a magnet and was frozen using a freeze-dryer (Freeze-dryer, Alfa 2-4LDplus, Christ Co., Germany). The protocol included flash freezing in liquid N_2, freezing at -80°C under the vacuum pressure of 0.001 mBar and finally cooling at 4°C for 48 h.

2.2. Instruments and methodologies.

The dried magnetic CS-Fe_3O_4 MNPs powder was used in order to investigate their magnetic behavior using a vibrating sample magnetometer (Meghnatis Daghigh Kavir Co., Kashan Kavir, Iran) with an applied field in the range of -8 and 8 kOe at 298 K. Fourier transform infrared (FTIR) spectrum of dried and purified magnetic nanoparticles was recorded in KBr pellets by a Bruker 113V FT-IR spectrometer. The structure of CS-Fe_3O_4 MNPs was characterized by one-dimensional wide-angle X-ray diffraction (XRD), which the pattern was recorded on Siemens D-500 X-ray diffractometer at a wavelength of λ=1.54 Å (Cu-K α), at a tube voltage of 35 kV, and tube current of 30 mA. Dried nanoparticles were coated with a thin layer of gold and studied using a scanning electron microscope-energy dispersive X-ray instrument (SEM/EDX, VEGAII, XMU, Czech Republic). The powdered nanoparticles were dispersed in distilled water and transmission electron microscope (TEM) micrographs were taken with a Philips CM10 operating at 60 kV tension. The average of particle size and size distribution were determined by dynamic light scattering (DLS) using a photon correlation spectroscopy (PCS) assembly with a malvern zetasizer (Malvern Instruments Limited, UK).

2.3. Preparation of seeds for germination.

2.3.1. Seed germination in Petri dish. Seeds of sweet pepper (*C. annum*) were purchased from Pakan Bazr Isfahan Co., Iran. The seeds were drained under running water for one hour. They were sterilized with a 2.5 % solution of sodium hypochlorite for 5 min and then rinsed 3 times with distilled water. Then, 40 seeds were transferred to Petri dishes containing the moistened filter paper (with 5 ml of distilled water or NPs solution) and were incubated at 25 ± 20°C in the light. The number of germinated seeds was determined every five day during the 20-day-long examination. Seed germination speed was calculated regarding the proportion of the total germinated seeds. Mean germination speed (R) was measured by equation (1) according to a previous report [42].

$$R=\sum Ni/\sum(Di*Ni) \quad (1)$$

Where Ni is the number of germinated seeds on day D, Di is the number of days counted from the beginning of the test.

2.3.2. Seed germination on paper towel. The paper towels were soaked in 5 ml of distilled water or NPs solutions (200, 400, 800 and 1600 mg/kg). After sterilization of seeds, they were located between two moist paper towels. The paper towels were covered with nylon coats and incubated at 25 ± 20°C in the dark. After 20 days seedlings were harvested. Shoot length (distance from the shoot tip to the collar zone), root length (distance from the root tip to the collar zone) and fresh and dry weights of vegetative organs were measured. The whole experiment was repeated three times.

2.4. Total iron content.

A quantity of 0.5 g of root and shoot tissues were weighed and dried. After powdering, the samples were digested using 11 mL mixed solutions of HNO_3- $HClO_4$ (10:1 ratio) at 100°C for 4 h in a tube-chamber microwave digestion system. The samples were filtered and diluted to 50 mL using distilled water. Then, concentrations of Fe in the digested tissues were determined by an ICP-OES atomic absorption spectrophotometer.

2.5. Imaging methods.

Epifluorescence microscopy was used to ensure the entry of Fe_3O_4 and chitosan-Fe_3O_4 MNPs into the treated plants. Observation of the control and treated plants was performed 5 days after the commencement of treatment. A number of roots of the plants were randomly selected and stained by Auramine O (0.1 % in 100 mL water) for 5 min. The samples were observed using an Olympus BX51 fluorescence microscope. The microscope was armed with the catadioptric lenses UMPlan FL-BDP and the BX-

RFA (Olympus Optical Co., Ltd. Tokyo, Japan) fluorescence illuminator. The best fluorescent shots were taken when U-MWB3 (480–510 nm) and U-MWG3 (510–550 nm) mirror cube units were used. The depth of field was enhanced by the stack z-projection to exert the final superimposed images [43, 44].

2.6. Statistical analysis.

Treatments were arranged in a completely randomized design with three replications. In order to detect significant differences between the treatments, the analysis of variance was employed. The multiple ranges Duncan's test was used to compare the treatment means using SAS version 9.1.

3. RESULTS SECTION

3.1. Characterization of nanoparticles.

The magnetic hysteresis loop of the magnetic CS-Fe_3O_4 was measured using VSM technique at ±9 kOe and 298 K. The CS-Fe_3O_4 sample demonstrated superparamagnetic behavior, which was evident from zero value for the coercivity and remanence on the magnetization curve (Figure 1). The saturation magnetization (Ms) of magnetic CS-Fe_3O_4 was obtained to be 29.1 emu/g. Compared to the pure Fe_3O_4 MNPs, the CS-Fe_3O_4 MNPs showed low Ms Value, which was assigned to the non-magnetic behavior of chitosan [45]. On the other words, because the saturation magnetization of materials is reported per g of sample, the Ms Value was gained lower for CS-Fe_3O_4 MNPs due to the presence of chitosan.

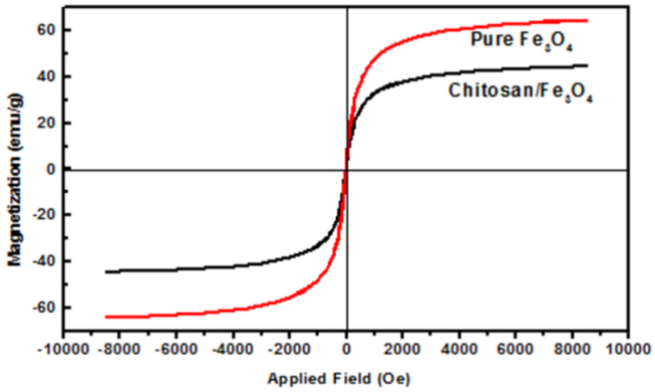

Figure 1. VSM curves of bare Fe_3O_4 and CS- Fe_3O_4 MNPs.

The chemical structure of CS-Fe_3O_4 MNPs was confirmed using FTIR and XRD techniques. The FTIR of chitosan showed characteristic bands at 1656, 1591, and 1070 cm^{-1} related to the amide I, amide II, and glycosidic bonds, respectively (Figure 2). The FTIR analysis of CS-Fe_3O_4 MNPs revealed a characteristic band at 575 cm^{-1}. This band was attributed to the Fe-O stretching vibrations, indicating the successful synthesis of Fe_3O_4 MNPs. Amid I bond of chitosan showed no shifting and its corresponding bond appeared at 1656 cm^{-1}. The amide II and glycosidic bonds of chitosan showed a shifting to a lower frequency (1550 and 1057 cm^{-1}, respectively), confirming the chitosan and Fe_3O_4 interaction.

The XRD patterns of chitosan and CS-Fe_3O_4 MNPs have further confirmed the formation of Fe_3O_4 nanoparticles. Pure chitosan sample showed a diffraction peak at $2\theta=20.42^{\circ}$, which corresponds to the partial crystalline structure of chitosan. The X-ray diffraction pattern of CS-Fe_3O_4 nanoparticles was shown in Figure 3. The main distinctive peaks of XRD appear at 2θ=30.5, 35.7, 43.3, 53.7, 57.6, and 63.1° which are related to the (220), (311), (400), (422), (511), and (440) plans of magnetite Fe_3O_4 nanoparticles [46].

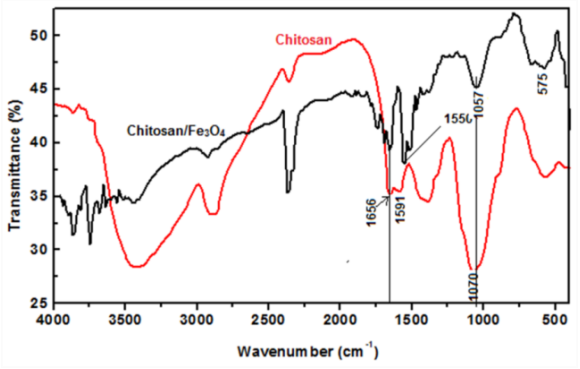

Figure 2. FT-IR spectra of CS and CS-Fe_3O_4 MNPs.

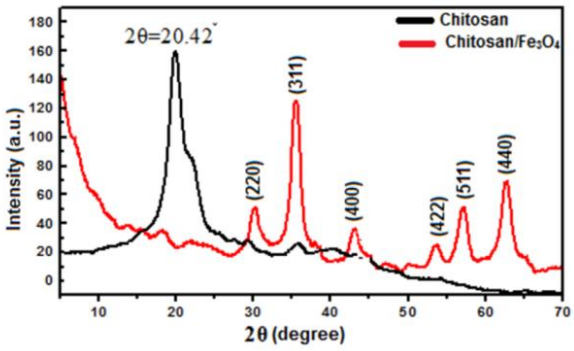

Figure 3. XRD patterns of CS and CS-Fe_3O_4.

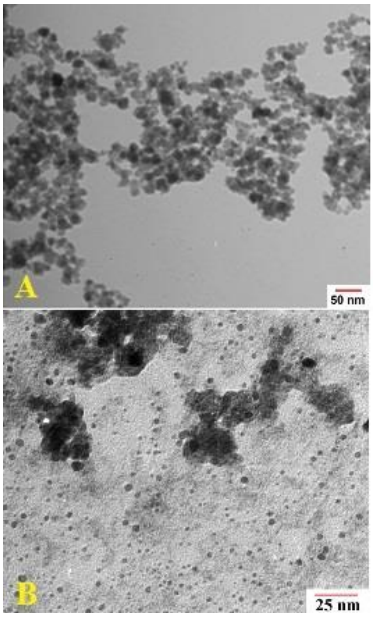

Figure 4. TEM images of (A) bare Fe_3O_4 and (B) CS-Fe_3O_4 MNPs.

The morphology of the bare Fe_3O_4 and CS-Fe_3O_4 MNPs were investigated by SEM and TEM techniques. According to the TEM images, the synthesized nanoparticles exhibited a well-defined spherical shape with a degree of aggregation (Figure 4 A, B). The sizes of bare Fe_3O_4 and CS-Fe_3O_4 nanoparticles were appeared to be in the range of 5-25 nm.

Based on the SEM images (Figure 5 A, B), the magnetic nanoparticles had a higher particle size (~45-90 nm) compared to the TEM result. The difference in the size of nanoparticles obtained by TEM and SEM techniques may be attributed to the loss of stability and aggregation of nanoparticles during the freeze-drying process [47].

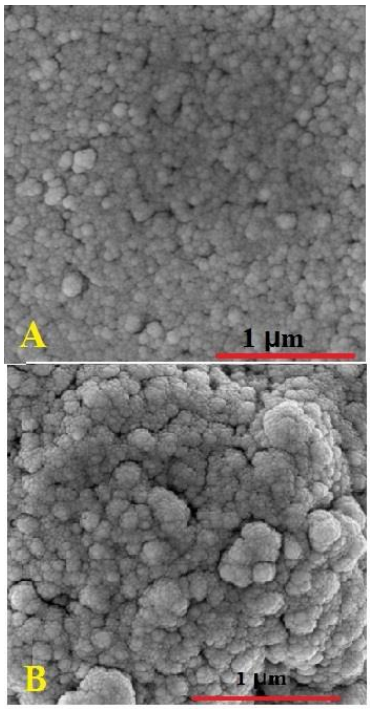

Figure 5. SEM images of (A) bare Fe_3O_4 and (B) CS-Fe_3O_4 MNPs.

DLS analysis was used to specify the hydrodynamic diameters of the magnetic nanoparticles. Figure 6 A and B depicted DLS analysis of bare Fe_3O_4 and CS-Fe_3O_4 MNPs in which the average diameters of ~ 66±3 nm and ~70±5 nm were obtained, respectively. Compared to the TEM results, the increase in the average size obtained from DLS data may be attributed to the aggregation of nanoparticles in solution [48].

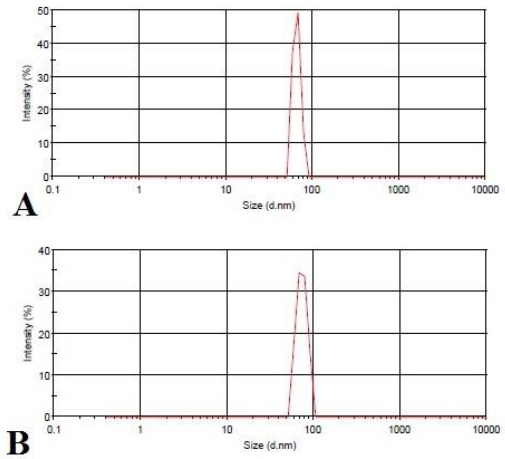

Figure 6. DLS diagrams of (A) bare Fe_3O_4 and (B) CS-Fe_3O_4 MNPs.

3.2. Fluorescence microscopic imaging.

To assess the entrance and localization of Fe_3O_4 and CS-Fe_3O_4 MNPs into the root tissues, treated plants were investigated by fluorescence microscopy. Obtained fluorescence microscopic images of treated plants verified the presence of Fe_3O_4 and CS-Fe_3O_4 MNPs as black spots and shiny green dots in root tissues, respectively (Figure 7 B, C.). In contrast, the images did not display any sign in the control specimens (Figure 7 A). The existence of shiny green spots could be related to CS around the Fe_3O_4 MNPs. These findings were in fair agreement with the previous reports on other plants [22, 49].

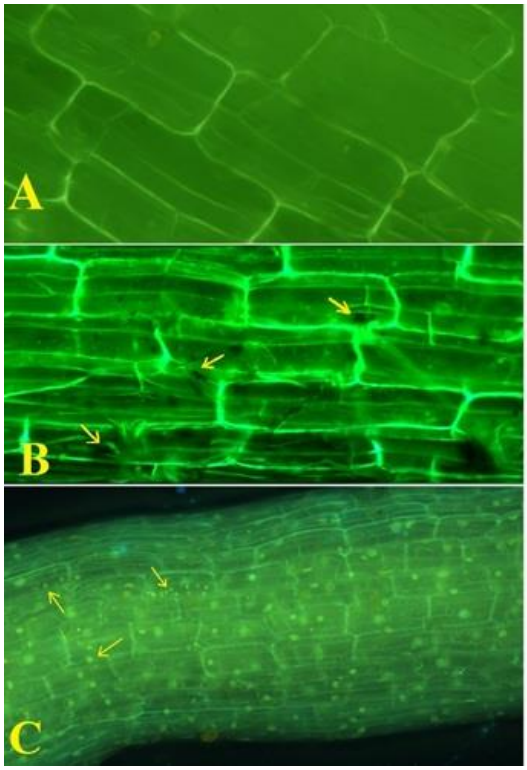

Figure 7. Fluorescence microscopic images of *C. annum* roots. Control groups (A) did not show any sign of MNPs in root cells. B and C illustrate the Fe_3O_4 and CS-Fe_3O_4 MNPs uptake and accumulation in root tissues, respectively. Dark spots demonstrate Fe_3O_4 MNPs aggregation and shiny green dots demonstrate CS-Fe_3O_4 MNPs accumulation inside the cells (arrows).

3.3. Germination and seedling growth parameters.

In this study, two different culture methods using Petri dishes and paper towels were used to evaluate the effects of different concentrations of Fe_3O_4 and CS-Fe_3O_4 MNPs on pepper seed germination and seedling growth.

3.3.1. Petri dish cultures. Different concentrations of Fe_3O_4 and CS-Fe_3O_4 MNPs had significant effects on germination of pepper seeds in Petri dishes. The low concentrations of the synthesized nanoparticles stimulated seed germination and the increasing concentration of nanoparticles led to a decrease in seed germination (Figure 8). Accordingly, the highest germination speed was observed in the seeds treated with 400 mg/kg Fe_3O_4 MNPs and 200, 400 mg/kg Cs-Fe_3O_4 MNPs (Figure 9 A). Moreover, Fe_3O_4 MNPs with 1600 mg/kg exhibited the lowest seed germination speed.

Compared to the control groups, low concentrations (200 and 400 mg/kg) of both Fe_3O_4 and CS-Fe_3O_4 MNPs showed the maximum germination percentage. Fe_3O_4 MNPs with highest

concentrations (800 and 1600 mg/kg) demonstrated the lowest percentage of germination (Figure 9 B).

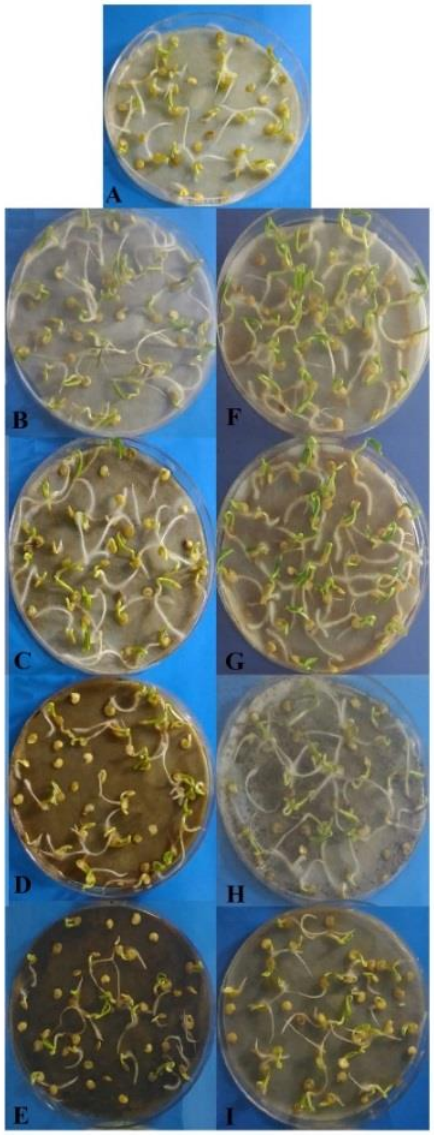

Figure 8. Effects of Fe_3O_4 and CS-Fe_3O_4 MNPs on seed germination of sweet pepper (A) control (B-E) Fe_3O_4 MNPs (200, 400, 800, 1600 mg/kg) and (F-I) CS-Fe_3O_4 MNPs (200, 400, 800, 1600 mg/kg).

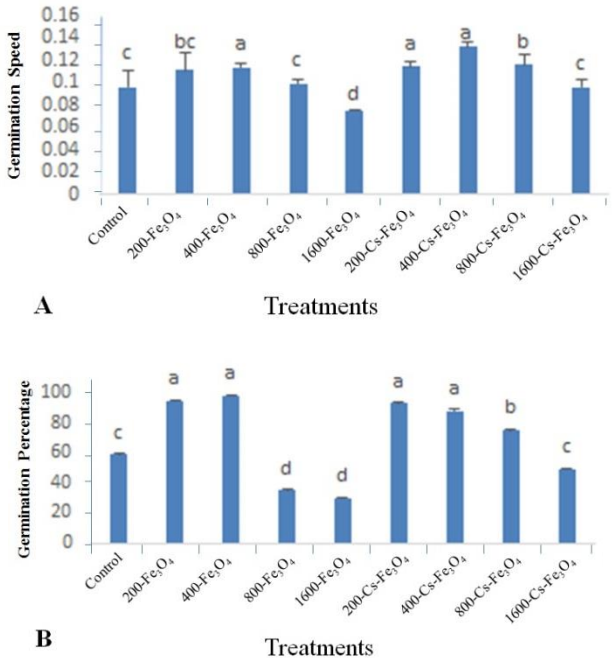

Figure 9. Effects of Fe_3O_4 and CS-Fe_3O_4 MNPs treatments on (A) seed germination speed and (B) germination percentage of pepper seeds in Petri dishes.

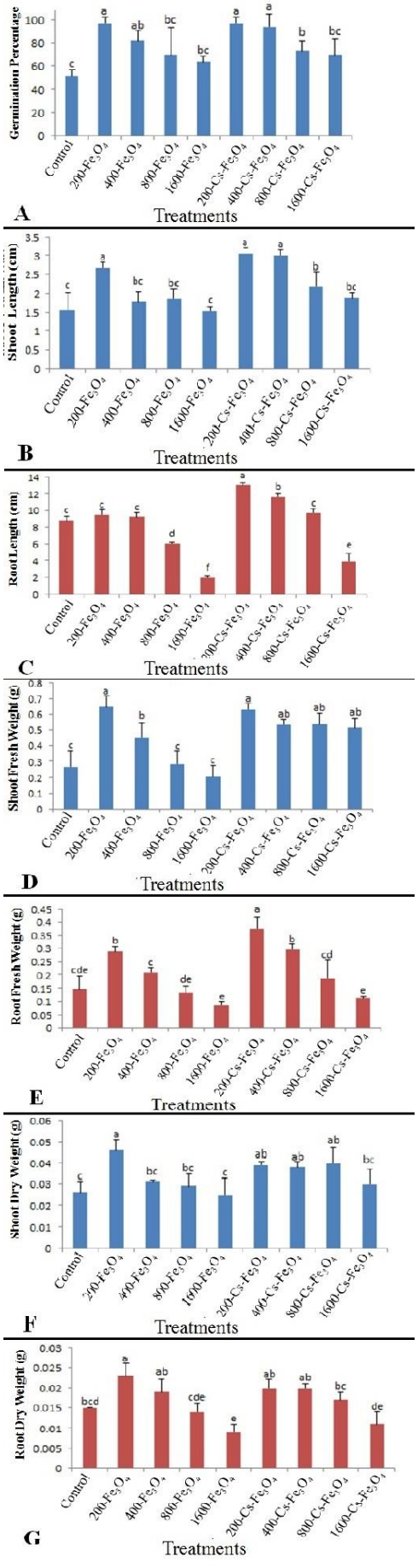

Figure 10. Effects of Fe_3O_4 and CS-Fe_3O_4 MNPs treatments on (A) seed germination, (B-C) plantlet length and (D- G) seedling biomass.

3.3.2. Culture in paper towel. To study the seedling growth parameters, we used paper towels culture; because the method provides appropriate moisture for seeds. Germination data using paper towels indicated that low concentrations of both types of nanoparticles had stimulating effects on germination rate (Figure 10 A-G). However, the lowest germination rate was observed in the control groups. (Figure 10, A). Growth indices of pepper seedlings significantly changed in different concentrations of Fe_3O_4 and CS-Fe_3O_4 MNPs. The highest length of shootlet was observed in the seedlings fed with 200 mg/kg of Fe_3O_4 MNPs and 200, 400 mg/kg of CS-Fe_3O_4 MNPs. In comparison, the lowest length of shootlet was observed in the seedlings exposed to 1600 mg/kg Fe_3O_4 MNPs (Figure 10, B).

Plant root is the first organ that directly exposed to nanoparticles and its growth reflects the plant's response to environmental conditions [9, 50, 51]. Exposing of pepper seedlings to 200 mg/kg of Cs-Fe_3O_4 and 1600 mg/kg of Fe_3O_4 MNP solutions led to the highest and the lowest lengths of rootlets, respectively. Low concentrations of both MNPs had positive effects on shootlet growth, but only in the highest concentration of Fe_3O_4 MNPs negative effects were observed (Figure 10, C). The seedling biomass was affected by use of different concentrations of nanoparticles. The highest amount of fresh weight of seedling was observed at 200 mg/kg of Cs-Fe_3O_4 concentration, while the lowest fresh weight was obtained in seedlings fed with highest concentrations of both nanoparticles (Figure 10, D-E). The seedlings treated with low concentrations of CS-Fe_3O_4 (200 and 400 mg/kg) and 200 mg/kg of Fe_3O_4 MNP showed the highest amount of dry weight. Remarkable negative effects on seedling dry weight were detected after treatment with the highest concentrations of both nanoparticles (Figure 10, F-G).

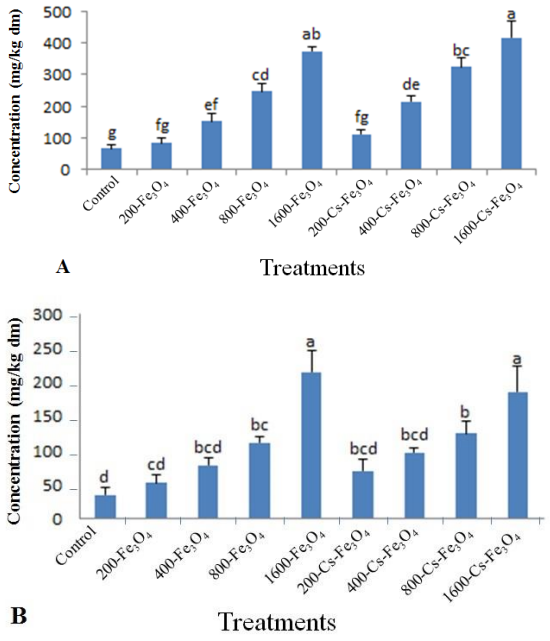

Figure 11. Total iron content in shootlets and rootlets of pepper plants treated with different concentrations of Fe_3O_4 and CS-Fe_3O_4 MNPs.

In the application of mineral compounds as plant nutrients, it is crucial to detect the threshold of toxicity. Germination speed, root growth, and more importantly root length are important indices in the diagnosis and evaluation of plant toxicity [15, 20, 25, 52]. Metal oxide nanoparticles may have inhibitory effects on different stages of plant growth, such as seed germination and root growth. For the evaluation of a wide range of xenobiotics toxicity, the percentage of germination could be considered as a fundamental index [20].

In this study, low and high concentrations of nanoparticles had stimulant and inhibitory effects on seed germination, respectively. Our results are in good agreement with other reported studies. For instance, stimulant effects of low concentrations of Fe_3O_4 MNPs were observed on mung bean, lettuce, cucumber, tomato seed germination without any signs of toxicity [16, 24, 53]. In contrary, two different concentrations (2000 and 5000 mg/kg) of Fe_3O_4 MNPs were reported to have remarkable inhibitory effects on seeds germination of *Linum usitatissimum*, *Lolium perenne* and *Hordeum vulgare* [25]. In addition, the application of Fe_3O_4 MNPs reduced the germination of wheat and rice seeds [54, 55].

It is well-known that the concentration of nanoparticles may influence the longitudinal growth of plant roots. Such a relationship was also observed in our studies. When we used the low concentrations of MNPs, the root growth was stimulated clearly. The similar results were reported on pumpkin and ryegrass using 30,100 and 500 mg/L Fe_3O_4 MNPs [56]. By applying the high concentrations of both synthesized-MNPs in our experiments, the root growth of pepper plants was inhibited. Generally, after seed germination, rootlets contact directly with iron oxide MNPs which covered the surface of roots and decreased the root growth [9, 51, 57]. Therefore, toxicity symptoms were more common in the roots [58]. The toxicity effects of Fe_3O_4 MNPs on roots have been reported on *Arabidopsis* and mango plantlets [52, 53]. In the present study, we observed short, branched and shrunk root tips as significant toxicity symptom using the high concentrations of Fe_3O_4 and CS-Fe_3O_4 MNPs. These results are also in agreement with the findings of a number of previous studies [59, 60].

3.4. Total Fe content in pepper seedlings.

Iron plays an important role in the structure and function of several enzymes [61, 62]. Therefore, Fe-containing nanoparticles may accelerate the seed germination by triggering of metabolic processes [63]. The measurement of Fe in pepper plantlets demonstrated a significant relationship between the Fe_3O_4 and CS-Fe_3O_4 MNPs concentrations in solutions and Fe accumulation levels in roots and shoots (Figure 11). As a result, the iron content in the roots was higher than the shoots. There are several reports on the high accumulation of Fe in root tissues under Fe-excess conditions [64-66]. Remarkably, plantlets exposed to CS-Fe_3O_4 MNPs possessed higher contents of iron due to the positive effects of chitosan, which probably facilitate the sustainable release of iron [67-69].

4. CONCLUSIONS

In summary, bare Fe_3O_4 and chitosan-coated Fe_3O_4 MNPs were synthesized and characterized. The positive and negative effects of the synthesized nanoparticles were exposed on seed germination and seedling growth of *C. annuum*. The results

revealed that application of 200 and 400 mg/kg Cs-Fe_3O_4 MNPs were optimal for the growth of the pepper seedlings. Compared to Fe_3O_4 MNPs, it was shown that chitosan-coated Fe_3O_4 MNPs supply sustainable release iron, which contributes to positive effects on seed germination and plantlet growth in low concentrations. Additionally, high concentrations of nanoparticles had inhibitory effects in seed germination, biomass production, and rootlet growth.

5. REFERENCES

[1] Ozdemir S., Dede O.H., Koseoglu G., Electromagnetic water treatment and water quality effect on germination, rooting and plant growth on flower, *Asian Journal of Water, Environment and Pollution*, 2, 2, 9-13, **2005**.

[2] Steeves T.A. Sussex I.M., Patterns in plant development, *Nordic Journal of Botany*, Cambridge University Press, **1989**.

[3] Markovic V., Takac A., Ilin Z., Enriched zeolite as a substrate component in the production of pepper and tomato seedlings, *Hydroponics and Transplant Production*, 396, 321-328, **1994**.

[4] Eldin A.S., Effect of Magnetite Nanoparticles (Fe_3O_4) as Nutritive Supplement on Pear Saplings. *Sciences*, 5, 3, 777-785, **2015**.

[5] Sahayaraj K., Nanotechnology and plant biopesticides: an overview, in Advances in Plant Biopesticides, *Springer*, **2014**.

[6] Singh A., Singh N.B., Hussain I., Singh H., Singh S.C., Plant-nanoparticle interaction: an approach to improve agricultural practices and plant productivity, *International Journal Pharmaceutical Science Invention*, 4, 8, 25-40, **2015**.

[7] Seabra A.B., Durán N., Nanotoxicology of metal oxide nanoparticles, *Metals*, 5, 2, 934-975, **2015**.

[8] Zheng L., Zheng L., Hong F., Lu S., Liu C., Effect of nano-TiO2 on strength of naturally aged seeds and growth of spinach, *Biological Trace Element Research*, 104, 1, 83-91, **2005**.

[9] Lin D., Xing B., Phytotoxicity of nanoparticles: inhibition of seed germination and root growth, *Environmental Pollution*, 150, 2, 243-250, **2007**.

[10] Adhikari T., Kundu S., Biswas A.K., Tarafdar J.C., Rao A.S., Effect of copper oxide nano particle on seed germination of selected crops, *Journal of Agricultural Science and Technology*, 2, 6A, 815, **2012**.

[11] de la Rosa G., López-Moreno M.L., de Haro D., Botez C.E., Peralta-Videa J.R., Gardea-Torresdey J.L., Effects of ZnO nanoparticles in alfalfa, tomato, and cucumber at the germination stage: root development and X-ray absorption spectroscopy studies, *Pure and Applied Chemistry*, 85, 12, 2161-2174, **2013**.

[12] Konate A., He X., Zhang Z., Ma Y., Zhang P., Alugongo G.M., Rui Y., Magnetic (Fe_3O_4) nanoparticles reduce heavy metals uptake and mitigate their toxicity in wheat seedling, *Sustainability*, 9, 5, 790, **2017**.

[13] Ren H-X., Liu L., Liu C., He S.Y., Huang J., Li J.L., Zhang Y., Huang X.J., Gu N., Physiological investigation of magnetic iron oxide nanoparticles towards chinese mung bean, *Journal of Biomedical Nanotechnology*, 7, 5, 677-684, **2011**.

[14] Karlsson H.L., Gustafsson J., Cronholm P., Möller L., Size-dependent toxicity of metal oxide particles—a comparison between nano- and micrometer size, *Toxicology letters*, 188, 2, 112-118, **2009**.

[15] García A., Espinosa R., Delgado L., Casals E., Acute toxicity of cerium oxide, titanium oxide and iron oxide nanoparticles using standardized tests, *Desalination*, 269,1-3, 136-141, **2011**.

[16] Barrena R., Casals E., Colón J., Font X., Evaluation of the ecotoxicity of model nanoparticles, *Chemosphere*, 75, 7, 850-857, **2009**.

[17] El-Yazied A., Shalaby O., El-Gizawy A., Khalf S., Effect of magnetic field on seed germination and transplant growth of tomato, *Journal of American Science*, 7, 12, 306-312, **2011**.

[18] Carbonell M., Florez M., Martínez E., Maqueda R., Amaya J.M., Study of stationary magnetic fields on initial growth of pea (*Pisum sativum* L.) seeds, *Seed Science and Technology*, 39,3, 673-679, **2011**.

[19] Stange B., Rowland R.E., Rapley B.I., Podd J.V., ELF magnetic fields increase amino acid uptake into *Vicia faba* L. roots and alter ion movement across the plasma membrane, *Bioelectromagnetics*, 23, 5, 347-354, **2002**.

[20] Lebedev S., Korotkova A., Osipova E., Influence of FeO nanoparticles, magnetite Fe_3O_4 nanoparticles, and iron (II) sulfate ($FeSO_4$) solutions on the content of photosynthetic pigments in *Triticum vulgare*, *Russian Journal of Plant Physiology*, 61, 4, 564-569, **2014**.

[21] Pariona N., Martínez A.I., Hernandez-Flores H., Clark-Tapia R., Effect of magnetite nanoparticles on the germination and early growth of *Quercus macdougallii*, *Science of the Total Environment*, 575, 869-875, **2017**.

[22] Ghafariyan M.H., Malakouti MJ., Dadpour MR., Stroeve P., Mahmoudi m., Effects of magnetite nanoparticles on soybean chlorophyll, *Environmental Science & Technology*, 47, 18, 10645-10652, **2013**.

[23] Iannone M.F., Groppa M.D., de Sousa M.E., van Raap M.B.F., Impact of magnetite iron oxide nanoparticles on wheat (*Triticum aestivum* L.) development: evaluation of oxidative damage, *Environmental and Experimental Botany*, 131, 77-88, **2016**.

[24] Giordani T., Fabrizi A., Guidi L., Natali L., Giunti G., Response of tomato plants exposed to treatment with nanoparticles, *EQA-International Journal of Environmental Quality*, 8, 8, 27-38, **2012**.

[25] El-Temsah Y.S., Joner E.J., Impact of Fe and Ag nanoparticles on seed germination and differences in bioavailability during exposure in aqueous suspension and soil, *Environmental Toxicology*, 27, 1, 42-49, **2012**.

[26] Mushtaq Y.K., Effect of nanoscale Fe_3O_4, TiO_2 and carbon particles on cucumber seed germination, *Journal of Environmental Science and Health*, Part A, 46, 14, 1732-1735, **2011**.

[27] Khataee A., Movafeghi A., Mojaver N., Vafaei F., Tarrahi R., Dadpour M.R., Toxicity of copper oxide nanoparticles on *Spirodela polyrrhiza*: assessing physiological parameters, *Research on Chemical Intermediates*, 43, 2, 927-941, **2017**.

[28] Mahjouri S., Movafeghi A., Divband B., Kosari-Nasab M., Kazemi E.M., Assessing the toxicity of silver nanoparticles in cell suspension culture of *Nicotiana tabacum*, *Biointerface Research in Applied Chemistry*, 8, 3, 3252-3258, **2018**.

[29] Movafeghi A., Khataee A., Abedi M., Tarrahi R., Dadpour M., Vafaei F., Effects of TiO_2 nanoparticles on the aquatic plant Spirodela polyrrhiza: Evaluation of growth parameters, pigment contents and antioxidant enzyme activities, *Journal of Environmental Sciences*, 64, 130-138, **2018**.

[30] Tarrahi R., Khataee A., Movafeghi A., Rezanejad F., Toxicity of ZnSe nanoparticles to *Lemna minor*: Evaluation of biological responses, *Journal of Environmental Management*, 226, 298-307, **2018**.

[31] Durán N., Seabra A.B., Metallic oxide nanoparticles: state of the art in biogenic syntheses and their mechanisms, *Applied Microbiology and Biotechnology*, 95, 2, 275-288, **2012**.

[32] Ingale A.G., Chaudhari A., Biogenic synthesis of nanoparticles and potential applications: an eco-friendly approach, *Journal of Nanomedicine and Nanotechnology*, 4, 165, 1-7, **2013**.

[33] Ahmadi Z., Akbari A., Mahdavinia, G.R., Encapsulation of *Satureja hortensis* L.(*Lamiaceae*) in chitosan/TPP nanoparticles with enhanced acaricide activity against *Tetranychus urticae* Koch (Acari: *Tetranychidae*), *Ecotoxicology and Environmental Safety*, 161, 111-119, **2018**.

[34] Sharif R., Mujtaba M., Ur Rahman M., Shalmani A., Ahmad H., Anwar T., The multifunctional role of chitosan in horticultural crops; A review, *Molecules*, 23, 4, 872, **2018**.

[35] Abdel-Aziz H., Hasaneen M.N., Omar A., Effect of foliar application of nano chitosan NPK fertilizer on the chemical composition of wheat grains, *Egyptian Journal of Botany*, 58, 1, 87-95, **2018**.

[36] Corradini E., De Moura M., Mattoso L., A preliminary study of the incorporation of NPK fertilizer into chitosan nanoparticles, *Express Polymer Letters*, 4, 8, 509-515, **2010**.

[37] Choudhary R.C., Kumaraswamy R.V., Kumari S., Sharma S.S., Pal A., Raliya R., Cu-chitosan nanoparticle boost defense responses and plant growth in maize (*Zea mays* L.), *Scientific Reports*, 7, 1, 9754, **2017**.

[38] Saharan V., Kumaraswamy R.V., Choudhary R.C., Kumari S., Pal A., Cu-chitosan nanoparticle mediated sustainable approach to enhance

seedling growth in maize by mobilizing reserved food, *Journal of Agricultural and Food Chemistry*, 64, 31, 6148-6155, **2016**.
[39] Aruna, A., Namasivayam S.K.R., Roy E.A., Comparative evaluation of non target toxic effect of free and polymer coated chemogenic metallic nanoparticles against *Vigna mungo*, *International Journal of Pharma and Bio Sciences*, 6, B461-B467, **2015**.
[40] Charles D.J., Antioxidant properties of spices, herbs and other sources, *Springer Science & Business Media*, **2012**.
[41] Arsalani N., Fattahi H., Nazarpoor M., Synthesis and characterization of PVP-functionalized superparamagnetic Fe_3O_4 nanoparticles as an MRI contrast agent, *Express Polymer Lett*ers, 4, 6, 329-38, **2010**.
[42] Ellis R., Roberts E., Improved equations for the prediction of seed longevity, *Annals of Botany*, 45, 1, 13-30, **1980**.
[43] Khataee A., Movafeghi A., Nazari F., Vafaei F., Dadpour M.R., Hanifehpour Y., Joo S.W., The toxic effects of l-cysteine-capped cadmium sulfide nanoparticles on the aquatic plant *Spirodela polyrrhiza*, *Journal of Nanoparticle Research* 16, 12, 2774-2783, **2014**.
[44] Tarrahi R., Khataee A., Movafeghi A., Rezanejad F., Gohari G., Toxicological implications of selenium nanoparticles with different coatings along with Se^{4+} on *Lemna minor*, *Chemosphere*, 181, 655-665, **2017**.
[45] Wu S., Ladani R.B., Zhang J., Kinloch A.J., Zhao Z., Ma J., Zhang X., Epoxy nanocomposites containing magnetite-carbon nanofibers aligned using a weak magnetic field, *Polymer*, 68, 25-34, **2015**.
[46] Dolatkhah A., Wilson L.D., Magnetite/polymer brush nanocomposites with switchable uptake behavior toward methylene blue, *ACS Applied Materials and Interfaces*, 8, 8, 5595-5607, **2016**.
[47] Feyzioglu G.C., Tornuk F., Development of chitosan nanoparticles loaded with summer savory (*Satureja hortensis* L.) essential oil for antimicrobial and antioxidant delivery applications, *LWT-Food Science and Technology*, 70, 104-110, **2016**.
[48] Römer I., White T.A., Baalousha M., Chipman K., Viant M.R., Lead J.R., Aggregation and dispersion of silver nanoparticles in exposure media for aquatic toxicity tests, *Journal of Chromatography A*, 1218, 27, 4226-4233, **2011**.
[49] Chitra K., Annadurai G., Synthesis and characterization of dye coated fluorescent chitosan nanoparticles, *Journal of Academia and Industrial Research*, 15, 199, **2012**.
[50] Shah F.U.R., *Heavy metal toxicity in plants, in Plant adaptation and phytoremediation*, Springer, **2010**.
[51] Yang Y., Wei X., Lu J., You J., Wang W., Shi R., Lead-induced phytotoxicity mechanism involved in seed germination and seedling growth of wheat (*Triticum aestivum* L.), *Ecotoxicology and Environmental Safety*, 73, 8, 1982-1987, **2010**.
[52] Lee C.W., Mahendra S., Zodrow K., Li D., Tsai Y.C., Braam J., Developmental phytotoxicity of metal oxide nanoparticles to *Arabidopsis thaliana*, *Environmental Toxicology and Chemistry*, 29, 3, 669-675, **2010**.
[53] Jayarambabu N., Kumari B.S., Rao K.V., Prabhu Y., Seed germination and growth parameters response of mungbean influence by biogenic Fe_3O_4 nanoparticles, *International Journal of Multidisciplinary Advanced Reserch Trends*, 1, 3, 34-40, **2017**.
[54] GR R., Sahoo S., Das A.B., Das S.R., Screening of iron toxicity in rice genotypes on the basis of morphological, physiological and biochemical analysis, *Journal of Experimental Biology*, 2, 6, **2014**.
[55] El Rasafi T., Nouri M., Bouda S., Haddioui A., The effect of Cd, Zn and Fe on seed germination and early seedling growth of wheat and bean, *Ekológia (Bratislava)*, 35, 3, 213-223, **2016**.
[56] Wang H., Kou X., Pei Z., Xiao J.Q., Shan X., Xing B., Physiological effects of magnetite (Fe_3O_4) nanoparticles on perennial ryegrass (*Lolium perenne* L.) and pumpkin (*Cucurbita maxima*) plants, *Nanotoxicology*, 5, 1, 30-42, **2011**.
[57] Kpongor D.S., Vlek P.L., Becker M., *Developing a standardized procedure to screen lowland rice (Oryza sativa) seedlings for tolerance to iron toxicity*, Technological and Institutional Innovations for Sustainable Rural Development, **2003**.
[58] Laxmi Verma N.P., The Effect of Iron Toxicity on Seed Germination and Early Seedling Growth of Green Gram (*Vigna radiata* L. Wilczek), *International Journal of Science and Research (IJSR)*, 6, 1427-1430, **2015**.
[59] Lin D., Xing B., Root uptake and phytotoxicity of ZnO nanoparticles, *Environmental Science and Technology*, 42, 15, 5580-5585, **2008**.
[60] Batty L., Younger P., Effects of external iron concentration upon seedling growth and uptake of Fe and phosphate by the common reed, *Phragmites australis* (Cav.) Trin ex. Steudel, *Annals of Botany*, 92, 6, 801-806, **2003**.
[61] Barberon M., Zelazny E., Robert S., Conéjéro G., Curie C., Friml J., Vert G., Monoubiquitin-dependent endocytosis of the iron-regulated transporter 1 (IRT1) transporter controls iron uptake in plants, *Proceedings of the National Academy of Sciences*, 108, 32, E450-E458, **2011**.
[62] Rout G.R., Sahoo S., Role of iron in plant growth and metabolism, *Reviews in Agricultural Science*, 3, 1-24, **2015**.
[63] Bastow E.L., de la Torre V.S.G., Maclean A.E., Green R.T., Merlot S., Vacuolar iron stores gated by NRAMP3 and NRAMP4 are the primary source of iron in germinating seeds, *Plant Physiology*, 00478, **2018**.
[64] Ma X., Geiser-Lee, J., Deng Y., Kolmakov A., Interactions between engineered nanoparticles (ENPs) and plants: phytotoxicity, uptake and accumulation, *Science of the Total Environment*, 408, 16, 3053-3061, **2010**.
[65] Hägnesten H., Zinc deficiency and iron toxicity in rice soils of Office du Niger, *Mali*, **2006**.
[66] Anchondo J., Wall M.M., Gutschick V.P., Smith D.W., Pigment accumulation and micronutrient concentration of iron-deficient chile peppers in hydroponics, *HortScience*, 36, 7, 1206-1210, **2001**.
[67] Dzung N.A., Khanh V.T.P., Dzung T.T., Research on impact of chitosan oligomers on biophysical characteristics, growth, development and drought resistance of coffee, *Carbohydrate Polymers*, 84, 2, 751-755, **2011**.
[68] Dzung N., Chitosan and their derivatives as prospective biosubstances for developing sustainable eco-agriculture, *Advances in Chitin Science*, 10, 453-459, **2007**.
[69] Muzzarelli R.A., Potential of chitin/chitosan-bearing materials for uranium recovery: An interdisciplinary review, *Carbohydrate Polymers*, 84, 1, 54-63, **2011**.

6. ACKNOWLEDGEMENTS

The authors would like to thank the University of Tabriz (Iran) and the University of Maragheh (Iran) for financial supports.